Project information	
Project full title	EuroSea: Improving and Integrating European Ocean Observing and Forecasting Systems for Sustainable use of the Oceans
Project acronym	EuroSea
Grant agreement number	862626
Project start date and duration	1 November 2019, 50 months
Project website	https://www.eurosea.eu

Deliverable information	
Deliverable number	5.4
Deliverable title	**CMEMS downscaled wave operational forecast system**
Description	This document describes the numerical modelling work for waves done in wp5.2. needed to implement OSPAC
Work Package number	WP5
Work Package title	Coastal Resilience and Operational Services Demonstrator
Lead beneficiary	UPC
Lead authors	Manuel Espino (UPC)
Contributors	Ivan Federico (CMCC), Salvatore Causio (CMCC), and Giovanni Coppini (CMCC), Maria Liste (UPC), Marc Mestres (UPC), Agustín S.-Arcilla (UPC), Marcos García Sotillo (EPPE), Manuel García León (EPPE), Enrique Álvarez-Fanjul (EPPE)
Due date	31 October 2021
Submission date	3 November 2021
Resubmission date	18 August 2023
Comments	This document was submitted 3 days late due to a formal revision.

This project has received funding from the European Union's Horizon 2020 research and innovation programme under grant agreement No. 862626.

https://doi.org/10.3289/eurosea_d5.4

Table of contents

Executive summary 1

1. Introduction 1

2. Areas of Interest 2

2.1. Taranto 2

2.2. Barcelona 4

3. Methodology 5

3.1. Numerical models 5

Taranto 5

Barcelona 6

3.2. Grid generation and bathymetry interpolation 8

Taranto 8

Barcelona 8

3.3. Initial and Lateral boundary conditions. Forcings. 9

Taranto 9

Barcelona 9

3.4. Physical and numerical setting 9

Taranto 9

Barcelona 10

3.5. Results 11

Taranto 11

Barcelona 18

4. Conclusions 23

Taranto 23

Barcelona 23

References 24

References for Taranto subsections 24

References for Barcelona subsections 25

Executive summary

This document explains in detail the set-up and implementation of two numerical high-resolution wave models for the Taranto and Barcelona test cases, as expected in the EuroSea work plan. Both models are state-of-the-art and have been carefully validated. The operating services resulting will be in the core of the OSPAC product, the main deliverable of WP5.2.

The third pilot involved in the project, Alexandría, does not have models ready since this port, quite unexpectedly, failed to obtain the internally required permits to work on the project. Nevertheless, this is not a concerning delay since all methodologies are developed, and we will proceed to the modelling work once the substitute port is designated. At this moment, locations in Colombia or Madagascar are being studied. Contacts with local authorities are established, and a final decision will be made before the end of 2021.

1. Introduction

The ocean is an essential part of the planet that plays a crucial role in the global life system and provides vital human resources. Coastal zones are the most affected areas by direct anthropic pressures, and their management is very complex due to the multiple interconnected processes that occur there. Therefore, understanding the physical behaviour of coastal zones is vital to managing the main problems related to impacts and resource exploitation activities (Liste et al., 2021). In this coastal setting, ports and adjacent cities are one of the main anthropic infrastructures that generate economic wealth; the increase in maritime traffic has resulted in rapid growth in port activity. As Ports and Cities are affected by met-ocean conditions, especially extreme events, personalized real-time and forecast information on environmental conditions is needed to manage their growth. Wind, waves, and sea level are traditionally critical metocean parameters.

Supporting port and city activities requires accurate ocean forecasting systems; In response to this growing demand for continuous and updated met-ocean information, high-resolution models are being implemented in coastal areas, combined with in situ observations, are allowing a better understanding and characterization of the main hydrodynamic characteristics of these areas. As a result, operational physical oceanography is maturing quickly, and high-resolution wave modelling as an operational capability is now a fact.

In the framework of the EuroSea Project, the WP5 team has been working on developing a wave forecasting operational tool with enough resolution to solve the wave dynamics of restricted domains such as Barcelona's and Taranto's local coastal waters, harbours, and beaches. This deliverable describes the wave operational forecast systems in Barcelona's and Taranto's local coastal waters.

The report is organized as follows: Section 2 describes the study site. Section 3 describes the 3D modelling systems and setups. Finally, section 4 presents validations and results.

2. Areas of Interest

2.1. Taranto

The Area of Interest is focused on the Southern Adriatic and Northern Ionian seas of Mediterranean basin, with special zoom in the Gulf of Taranto (hereafter GT) and particularly in the Mar Grande and Mar Piccolo where the port of Taranto is located.

The southern Adriatic Sea extends approximately southward along the latitude of 42°N to the threshold of the Strait of Otranto and has a maximum depth of 1270 m. An exchange of waters with the Ionian Sea occurs at the Strait of Otranto at approximately 40°N. The northern Ionian Sea extends south of 38°N and has a steeper continental slope than the Adriatic basin. The offshore maximum depth is 3500–3700 m.

The GT (Figure 1a) is situated in the north-western Ionian Sea and is approximately delimited in open sea by the line connecting Apulia and Calabria (Gulf of Taranto – Boundary Section, GT-BS in Figure 1a). It is a deep, semi-enclosed ocean area in southern Italy encircled by two peninsulas, Apulia and Basilicata/Calabria (Figure 1a). It is open to the northern Ionian Sea, and a deep trench of more than 2000 m connects it to the eastern Mediterranean Sea. The continental shelf area, considered as the area from the coasts to the 200 m depth contour, occupies only 10 % of the total Gulf area (Pinardi et al., 2016) with the shelf wider on the Apulia than the Calabria side.

A 7.5 km wide sheltered elliptical embayment, called the Mar Grande – Mar Piccolo system of Taranto, see Figure 1b, hereafter named MG-MP), opens in the north-eastern part of the GT. The MG-MP is a marine system experienced over the last few decades strong biochemical pollution and environmental degradation, and it is considered a hotspot study site for economic, ecological and scientific reasons

Few studies are available on the wave climate of the Gulf of Taranto. Greco and Martino (2014) evaluated the main direction of the wave field off the Ionian western coast, performed by means of hindcasting method. The frequency of the sea state from SE direction is higher than 50%. Damiani et al. (2007) described the wave climate for the year 2006 using a buoy in proximity of the mouth of the Great Sea in Taranto. The buoy was moored about 1.5 km from Taranto at a location with a water depth of about 72 m, to measure sea states not altered by the interaction with bottom. They reported that the longest fetch is about 1400 km from the SSE. The recorded wave heights during the year analysed were relatively small and the maximum significant wave height was Hs = 2.88m (April 2006). The wave climate in the Gulf is characterized by a rather constant SSE direction. The waves come from a quite limited approaching sector and the wave field direction is very constant overall the year. The only remarkable change happens during the summer season when there is a greater occurrence of low height waves generated from local winds blowing from NW directions (Figure 2).

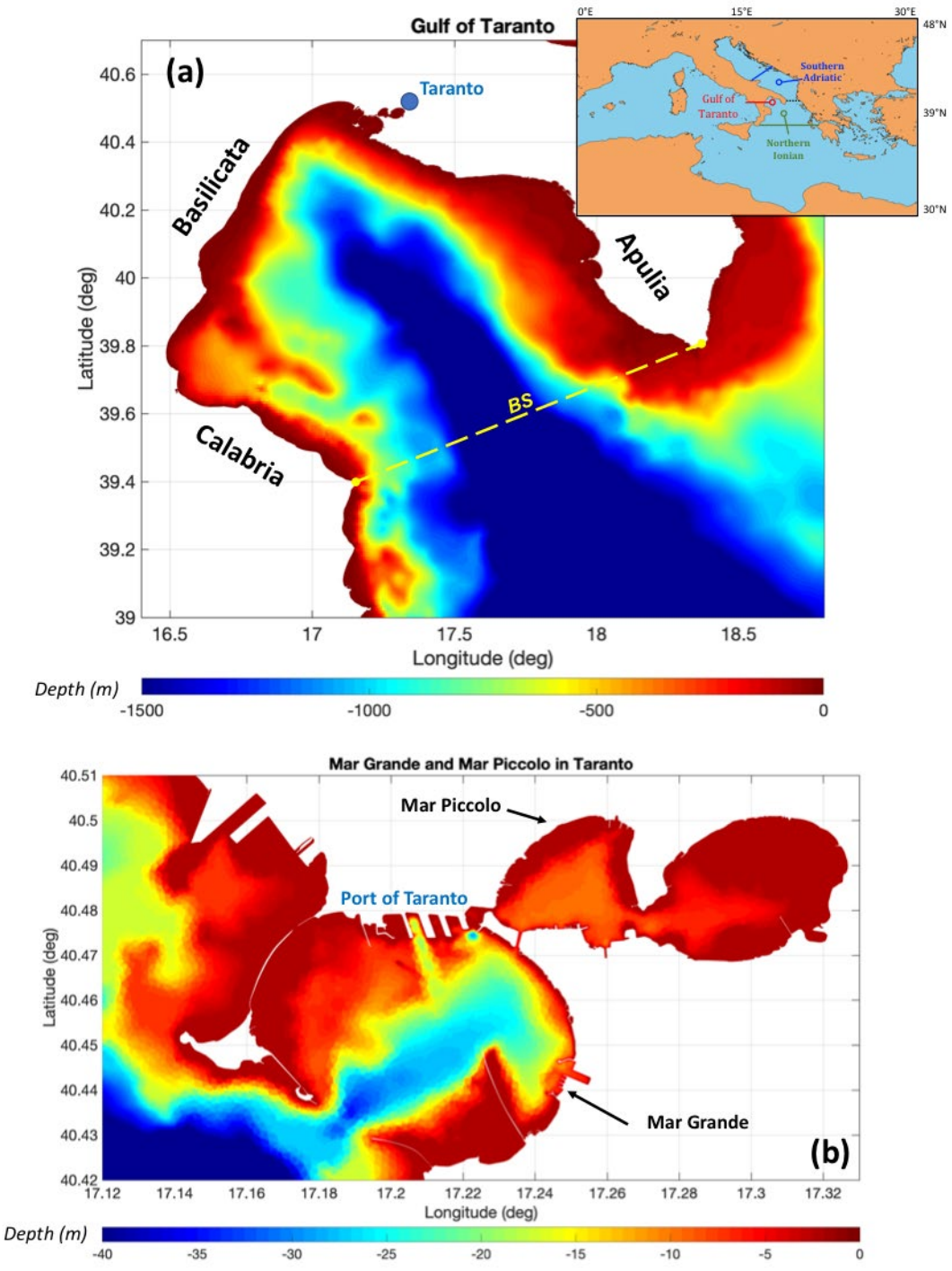

Figure 1. Area of interest: bathymetry and coastline of Gulf of Taranto (a) and Mar Grande (southwestern part of domain, where port of Taranto is located) and Mar Piccolo (northeastern part of domain) of Taranto (b)

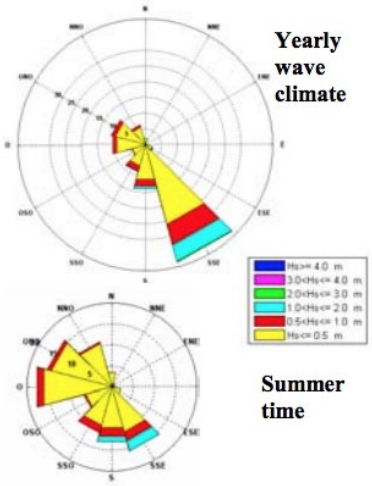

Figure 2. Mean wave climate for the Gulf of Taranto at yearly time-scale for the whole 2006 (top wave rose) and for seasonal time-scale (Summer 2006) from Damiani et a.,2007.

2.2. Barcelona

In particular, the study area is focused on the coastal waters and port of Barcelona city, located on the Catalan coast in the Northwest Mediterranean Sea (see Figure 3). It corresponds to the northern section of the Spanish coast, situated between latitudes 40°45' N and 42°25' N and longitudes 0°45' E and 3°15' E, with an extension of around 700 km (Pallares et al. 2014).

The general circulation pattern presents a relatively complex pattern primarily determined by the bottom bathymetry (Sánchez-Arcilla and Simpson, 2002). The characteristics of the continental shelf and the slope are crucial: in the north, the shelf is broad (about 70 km), narrows to less than 20 km in the central stretch of the coast (in front of Barcelona city), and then widens again abruptly to about 60 km further south. Due to the microtidal character of the Mediterranean Sea, tidal perturbations to the currents are not significant in this area (Poulain et al., 2013; Tsimplis et al., 1995).

Orographic patterns, air-sea temperature differences and the passage of low-pressure centres from the Atlantic mainly control the meteorological situation in the area. The Pyrenees, situated north of the Catalan coast, act as a physical barrier that modifies the wind patterns and produces the Mistral and the Tramontana, northwest and north winds, respectively, whose influence can be noticed hundreds of kilometres offshore (Bolaños et al., 2009). Also, the wind channelling due to river valleys and the complex topography generate highly variable wind patterns in space and time.
The prevalent winds come from the north and northwest, primarily during December and January; southerly and easterly winds are also significant, particularly during February, March, April and November (Arnau, 2000). On average, the winds are not very intense. The maximum velocities correspond to easterly winds in agreement with storm conditions. ; the most energetic storms registered in the area are associated with this directional sector and affect the entire length of the Catalan coast (Mendoza et al., 2011).

The predominant wave directions, as with the wind, vary along the coast showing clearly the topographic control due to a complex bathymetry, with submarine canyons and a heterogeneous continental shelf width (Sánchez-Arcilla et al., 2008; Bolaños et al., 2009). Sánchez- Arcilla et al. (2008) describe how waves from east and south are the prevailing wave conditions in the study area. The largest waves come from the east, where the largest fetches and stronger winds coincide (Pallares et al. 2014).

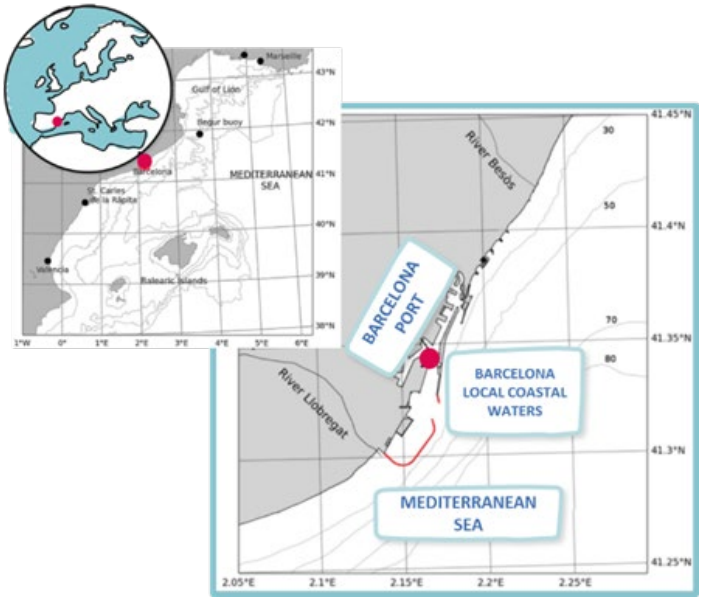

Figure 3. The upper left panel shows the extended study area comprising the NW Mediterranean. The central panel focuses on Barcelona's local coastal waters and port area. Isobaths are drawn up to 80m.

3. Methodology

3.1. Numerical models

Taranto

The modelling system is based on WAVEWATCH III™, a community wave modeling framework that includes the latest scientific advancements in the field of wind-wave modeling and dynamics.

The core of the framework consists of the WAVEWATCH III third- generation wave model, developed at the US National Centers for Environmental Prediction (NOAA/NCEP) in the spirit of the WAM model (Komen et al., 1984).

WAVEWATCH III, hereafter WW3 solves the random phase spectral action density balance equation for wavenumber-direction spectra. The implicit assumption of this equation is that properties of medium (water depth and current) as well as the wave field itself vary on time and space scales that are much larger than the variation scales of a single wave. The model includes options for shallow-water (surf zone) applications, as well as wetting and drying of grid points. Propagation of a wave spectrum can be solved using regular

(rectilinear or curvilinear) and unstructured (triangular) grids, individually or combined into multi-grid mosaics.

Source terms for physical processes include parameterizations for wave growth due to the actions of wind, exact and parametrized forms accounting for nonlinear resonant wave-wave interactions, scattering due to wave-bottom interactions, triad interactions, and dissipation due to whitecapping, bottom friction, surf-breaking, and interactions with mud and ice. The model includes several alleviation methods for the Garden Sprinkler Effect, and computes other transformation processes such as the effects of surface currents to wind and wave fields, and sub-grid blocking due to unresolved islands. Wave energy spectra are discretized using a constant directional increment (covering all directions), and a spatially varying wavenumber grid. First-, second- and third-order accurate numerical schemes are available to describe wave propagation. Source terms are integrated in time using a dynamically adjusted time stepping algorithm, which concentrates computational efforts in conditions with rapid spectral changes. The model is used worldwide by several institutions to simulate waves of several systems in many regions of the world, from global to coastal scale. The wave model has been interfaced in terms of coupling with SHYFEM circulation model (described in deliverable 5.3) via radiation stress theory (Longuet-Higgins and Stewart, 1964).

The modelling approach is based on the downscaling of CMEMS Marine products released at the regional scale of Mediterranean Sea. The current Med_Waves-CMEMS (Korres et al., 2021) implementation is based on WAM Cycle 4.6.2 with proper tuning and maximum spectral steepness limitation and it has been developed as a nested sequence of two computational grids (coarse and fine) to ensure that swell propagating from the North Atlantic towards the strait of Gibraltar is correctly entering the Mediterranean Sea. The coarse grid covers the North Atlantic Ocean from 75°W to 10°E and from 70°N to 10°S in 1/6° resolution while the nested fine grid covers the Mediterranean Sea from 18.125°W to 36.2917°E and from 30.1875°N to 45.9792°N with a 1/24° (~4.6km) resolution. The Med-Waves modelling system resolves the prognostic part of the wave spectrum with 24 directional and 32 logarithmically distributed frequency bins and the model solutions are corrected by an optimal interpolation data assimilation scheme of along-track significant satellite wave height observations. The system provides a Mediterranean wave analysis and 10 days Mediterranean wave forecasts updated twice a day.

Barcelona

Reliable knowledge of surface gravity waves, currents, and their interactions in the ocean is of great importance to many applications, such as weather forecasting, search and rescue, beach erosion, and site selections for offshore infrastructures (Hashemi and Neill, 2014). Waves and currents form a complex system usually discussed, assuming the influence of waves on hydrodynamics and the impact of currents on waves distinctly (Benetazzo et al., 2013). This broad topic is usually referred to with the general term of Wave–Current Interaction (WCI) that, from the general point of view, traces back to the theoretical works of Longuet-Higgins (1964) on longshore currents flows produced by waves and to the studies of the dynamics of waves in a moving medium (Tayfun et al., 1976). Physically, ocean currents can modify the relative speed of the air above the sea surface (relative wind effect) and change the absolute frequency of waves, known as the Doppler shift. In addition, spatial variability of currents can modify the relative wave frequency and cause wave refraction, shoaling, and breaking that mimic bathymetric effects (Ding and Wang, 2011). The surface

gravity waves, in return, can affect vertical mixing and surface and bottom stress experienced by currents. The surface waves and currents can also exchange energy through radiation stress (Stewart et al., 1974; Mellor, 2003) or vortex force (McWilliams et al., 2004; Ardhuin et al., 2008).

In the framework of the EuroSea initiative, the LIM-UPC team has developed a 3D hydrodynamic tool with enough resolution to solve the inner dynamics of local domains such as Barcelona's coastal waters, harbour, and beaches. The effect on waves of the Wave-Current Interaction (WCI) process in Barcelona's coastal waters and the port was investigated using the Coupled Ocean-Atmosphere-Wave-Sediment Transport (COAWST) modelling system. COAWST relies on the ocean model ROMS (Regional Ocean Modeling System) and SWAN (Simulating WAves Nearshore) wave model. The simulations are based on a two-way coupling between ROMS and SWAN on the same computational grids. The atmospheric forcing was uncoupled, and CMEMS products provided the fields.

Circulation model:

ROMS is a three-dimensional, free-surface, topography-following numerical model that solves finite difference approximations of Reynolds Averaged Navier Stokes (RANS) equations using hydrostatic and Boussinesq approximations with a split-explicit time-stepping algorithm (Shchepetkin and McWilliams, 2005; Haidvogel et al., 2008; Shchepetkin and McWilliams, 2009). In addition, ROMS includes options for various model components such as different advection schemes (second, third, and fourth-order), turbulence closure models (e.g., Generic Length Scale mixing, Mellor-Yamada, Brunt-Väisälä frequency mixing, user-provided analytical expressions, K-profile parameterization), and several options for boundary conditions.

We used the latest version of the ROMS model (version 3.9) at this deliverable's publication date. However, numerical details, a complete model description, user documentation, and source code are available on the ROMS website for future checks and improvements.

Wave model

SWAN is a state-of-the-art 3rd generation spectral wave model which computes random, short-crested wind-generated waves in offshore and coastal regions. The model describes the generation, evolution, and dissipation of the wave action density spectrum N (space, time; σ, θ), where θ is the wave propagation direction, and σ is the wave relative frequency. SWAN solves a radiative time-dependent transport equation in the variable N, accounting for the wind input, the wave-wave interactions, and the dissipation terms in deep and shallow waters. The ambient current affects the density spectrum balance in two ways. One way is that N will be propagated with a velocity modified by the local ocean current. A second way is that the effects of ocean currents are accounted for by using the apparent local wind speed and direction to modify the wind stress (Kara et al., 2007). The wind speed modification by the local currents is implemented in COAWST, assuming the atmosphere flow relative to a moving frame: the wind speed is shifted by the ocean current velocity (validations and limits provided by Hersbach and Bidlot, 2008).

We used the latest version of the SWAN model (version 41.31) at this deliverable's publication date. However, numerical details, a complete model description, user documentation, and source code are available on the SWAN website for future checks and improvements.

Coupling tool

The COAWST model utilizes the model-coupling toolkit (MCT) to achieve communication among the submodels via the message-passing interface (Jacob et al., 2005). In the coupling process, ROMS receives the surface and bottom wave direction, height, length, period, percentage breaking, energy dissipation, and bottom orbital velocity from SWAN. At the same time, ROMS provides bathymetry, bottom elevation, sea-surface height, and depth-averaged currents to SWAN.

We used the latest version of the COAWST modelling system (version 3.7) at this deliverable's publication date. However, complete model details are available on the COAWST website for detailed checks and future improvements.

3.2. Grid generation and bathymetry interpolation

Taranto

In EuroSea, we have developed a specific and hyper-resolution configuration for Taranto Seas, hereafter GT-WAVE. The new system covers only the GT with a horizontal resolution from 3 km in open-sea to 100 m in the coastal waters to 20 m in the port of Taranto. Figure 4 shows the grid and bathymetry in GT and MG-MP. A single open boundary is created connecting Calabria and Apulia coasts through the GT-BS (see Figure 1a). This configuration has been created to perform specific process studies and long-term hindcast simulations, due to the reduced density meshes in respect with the first one. The new horizontal grid has been created adopting advanced and customized tools (mainly python-based) of meshing based on GMSH[1] and BLENDER[2] software.

The bathymetry was derived from the EMODnet[3] product at a resolution of 1/8 x 1/8 arc-minutes (circa 230 x 230 meter), resolution for open sea and coastal waters and integrated with higher-resolution bathymetry (resolutions of order of meter) for coastal areas in MG-MP and Taranto Port area provided by the Italian Navy Hydrographic Institute. The wave spectra have been discretized in 24 directions (covering the full circle) and 32 frequencies, from 0.05 Hz to 0.9597 Hz.

Barcelona

Bathymetries are built using a combination of bathymetric data from EMODnet[4] and specific high-resolution sources provided by local Port Authorities (Figure 5). An updated and higher resolution bathymetry is also applied to adjust the open boundary to the coastal bathymetries in the port domains. Finally, the bathymetry information interpolated is smoothed using a Shapiro filter with an r-factor criterion below 0.25.

The bottom boundary layer was parameterized with a logarithmic profile using a characteristic bottom roughness height of 0.002 m. The turbulence closure scheme for the vertical mixing is the generic length scale (GLS) tuned to behave as k-epsilon (Warner et al., 2005). Horizontal harmonic mixing of momentum is defined with constant values of 5 m^2s^{-1}.

[1] http://gmsh.info/

[2] https://www.blender.org/

[3] https://www.emodnet-bathymetry.eu/

[4] https://emodnet.ec.europa.eu

3.3. Initial and Lateral boundary conditions. Forcings.

Taranto

The modelling system is downscaled from Med-Waves-CMEMS in term of open boundaries. The scalar fields from Med-Waves-CMEMS (significant wave surface height, peak wave period and mean direction) are treated at the boundary nodes of the nested system through the Yamaguchi, 1984 approximation, to rebuild local wave spectra.

The model is initialized using the fetch limited approach: the local JONSWAP spectrum is calculated using the local wind speed and direction, using the spatial grid size as fetch.

Meridional and zonal 10 m wind components (U10M and V10M) of well-consolidated atmospheric products from ECMWF (6.5 km resolution and 3h frequency) are adopted as forcing. The atmospheric fields are corrected by land-contaminated points following Kara et al. (2007) and horizontally interpolated at each ocean grid node by means of linear interpolation.

Barcelona

The model configuration is nested into the daily updated regional ocean forecast products delivered by CMEMS-IBI (Sotillo et al., 2015). At the sea surface, the models are driven by high frequency (hourly) wind stress, atmospheric pressure, and fluxes of water and surface heat derived from the Spanish Meteorological Agency (AEMET) forecast services, based on two operational applications of the HIRLAM (HIgh-Resolution Limited Area Model) model: one, the HNR application which is corresponded with the Iberic Peninsula geographic domain (0.05° resolution and a forecast horizon of + 36 h) and the ONR application which is corresponded with the Euro-Atlantic geographic domain (0.16° resolution and a forecast horizon of + 72 h). Further detailed information on this methodology can be found in Sotillo el et al. 2019.

The HNR and ONR fields are jointly used according to the best available basis and pre-processed to obtain wind surface stress, net surface heat, and salinity fluxes. CMEMS-IBI provides hourly barotropic water currents and sea level and is consistently applied as Open Boundary Conditions (OBC) with Chapman and Flather algorithms (Carter and Merrifield 2007). Moreover, daily average CMEMS-IBI currents, temperature, and salinity values are imposed through the water column as clamped (Dirichlet) boundary conditions (Sotillo et al., 2019).

3.4. Physical and numerical setting

Taranto

GT_WAVE has been implemented following WAM Cycle4 model physics (Günther et al. 1992). The propagation scheme used is a third order scheme (Ultimate Quickest) with "Garden Sprinkler Effect" alleviation method of spatial averaging. Wind input and dissipation are based on Ardhuin et al., 2010, in which the wind input parametrization is adapted from Janssen's quasi-linear theory of wind-wave generation (Janssen, 1991, Chalikov and Belevich, 1993), following adjustments performed by Bidlot et al. 2005 and Bidlot 2008. Nonlinear wave-wave interaction have been modelled using the Discrete Interaction Approximation (DIA) (Hasselmann et al. 1986, Hasselmann et al. 1985).

The model system includes shallow water physics for coastal processes. Nonlinear triad interactions are modelled using the LTA model of Eldeberky (1996). Depth-induced breaking has been implemented using the approach of Battjes and Janssen (1978).

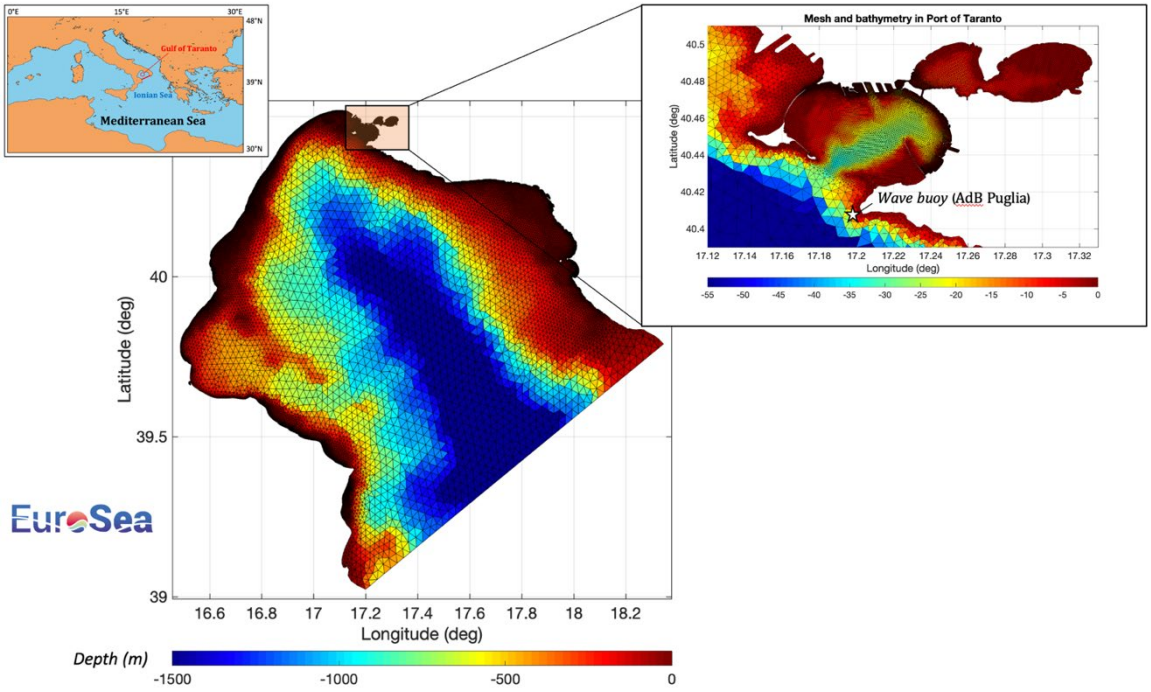

Figure 4. Horizontal grid with bathymetry overlapped for Gulf of Taranto system and for MG-MP. Star symbol indicates the wave buoy location (property of Autoritá di Bacino, Apulia region) used for validation.

Barcelona

The numerical simulations were performed on a coupled, two-nested grid configuration. The coarse grid covers part of the Catalan coast with a spatial resolution of 350m (Figure 5). Nested within the Coastal grid by a scale factor of 5 is the Port grid with a spatial resolution on the order of 70 m (Fig. 5). Two grids were simulated concurrently as a nested-coupled application: two-way ocean refinement and one-way wave refinement with fully coupled exchanges between two grids for the fields of water levels, currents, bathymetry, and bottom roughness from the ocean to the wave model; and wave dissipation, height, length, direction, surface and bottom periods, and bottom orbital velocities from the wave to the ocean model. The relevant ocean physics that include waves are surface-enhanced roughness due to the waves from Taylor and Yelland (2001), the surface-enhanced flux of turbulent kinetic energy due to wave breaking based on Craig and Banner (1994) with an increased roughness dependent on the sea state (Carniel et al., 2009), wave effects on currents as described in Kumar et al. (2012) based on the approach from Uchiyama et al. (2010), and the enhanced bottom roughness due to waves from Madsen (1994). The wave dynamics enhanced from coupling to the ocean model include the effects of varying bottom roughness, changes in water level, and effects from near-surface currents based on Kirby and Chen (1989).

Ocean model was forced with atmospheric data of winds, pressure, air temperature, relative humidity, precipitation, and heat fluxes from CMEMS-IBI. At the sea surface, the models were forced by high frequency

(hourly) wind stress, atmospheric pressure, and fluxes of water and surface heat derived from the Spanish Meteorological Agency (AEMET) forecast services.

The model grids were time stepped with 60 and 15 s (for Coastal and Port grids) for the ocean, and 30 and 15 s for the wave model.

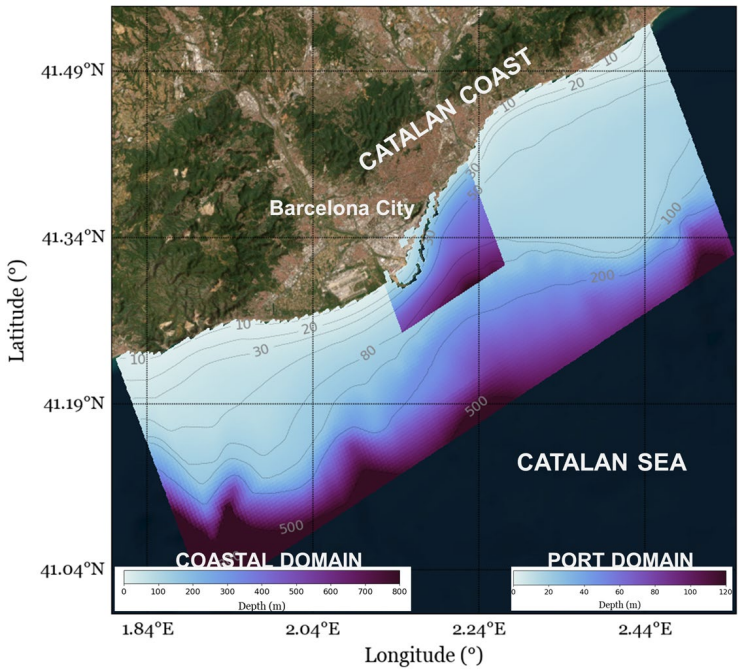

Figure 5. Horizontal grid with bathymetry overlapped for the Coastal domain and Port domain. Note that the colour scale for the bathymetry is different to visualize the Port domain grid within the Coastal domain grid.

3.5. Results

Taranto

Here we show results in the coastal and harbour scale of Taranto and a quantitative analysis comparing the modelling results with observations, especially during extreme wave events.

Figure 6 shows Significant Wave Height (Hs) over the entire model domain under downwind conditions (Easterly winds), with a zoom on the MG.

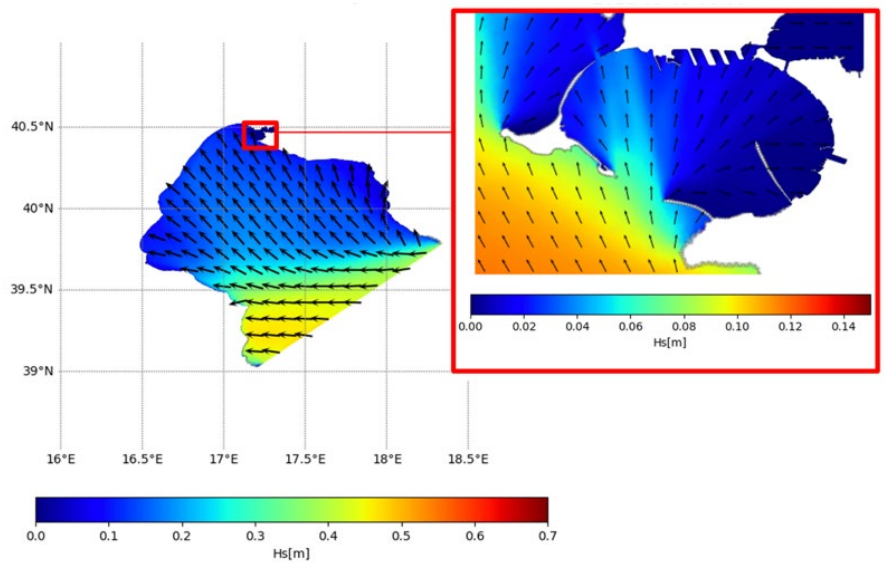

Figure 6. Significant wave height on the Gulf of Taranto (left panel) and on the MG (right panel) under downwind conditions.

Figure 7 shows a numerical experiment aimed to assess the impact on Hs and mean wave period (Tm) due the inclusion of shallow water physics in GT_WAVE. The top panels show the Hs and Tm for the full set-up (both deep and shallow water physics), while the bottom panel the difference between simulation using the full set-up and simulation based on only deep-water physics. In particular the Hs of full set-up is comparable to the one of only deep water set-up except for the coast, where shallow water physics are activated. The Hs reduction in full set-up experiment is estimated to be around ˜-15% close to the Isola di San Pietro coast. Similar behavior is reported for Tm.

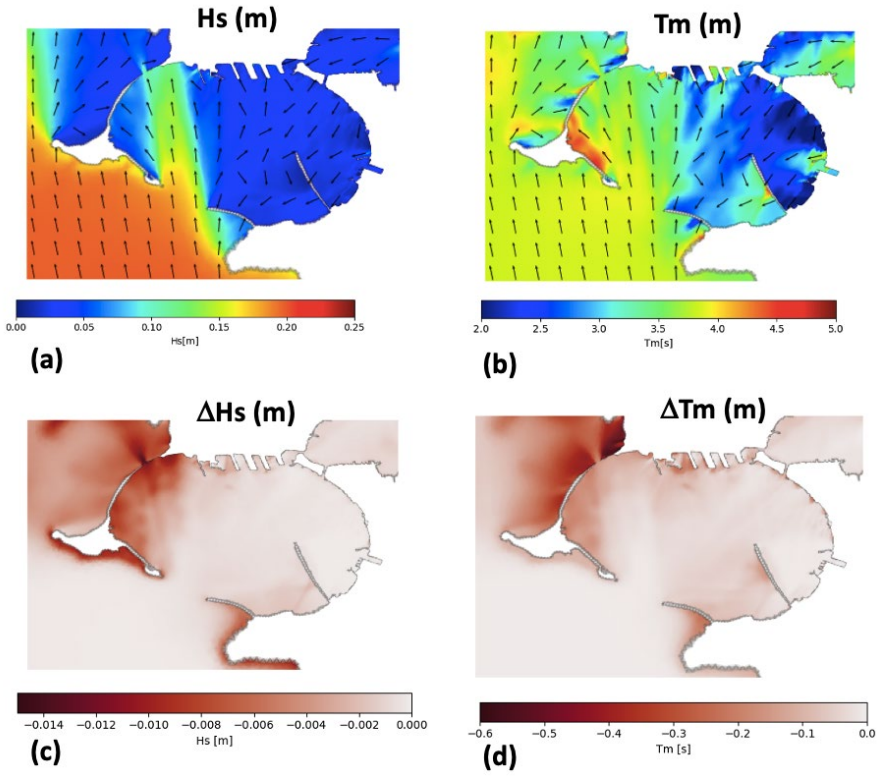

Figure 7. Significant wave height (a) and mean period (b) for GT-WAVE full set-up (both deep and shallow water physics). Difference between full set-up and only deep-water physics for significant wave height (c) and mean period (d).

In the next section we analyzed and validated the GT-WAVE implementation, considering three extreme events between 2014 and 2016, where data from buoys are available. The wave buoy data have been provided by the Autoritá di Bacino of Apulia region, and they were compared to Hs and Tm of GT-WAVE and its parent model (Med-Waves-CMEMS). The water depth where the buoy is located approximately at 72 m, thus we were able to validate only the deep-water physics of our implementation. The location of the buoy is reported in Figure 4.

The first event occurred in 2014, on 4-6 October. In Figure 8 we report the significant wave map at the highest peak of the event and the timeseries of Hs and Tm during the event. Two peaks of Hs (1.8m and 1.6m) are present, with a mean direction at the boundary from southeast. Both the peaks were better represented by GT-WAVE with respect to the CMEMS parent model. For the first peak it is evident an underestimation by both the models, while the second one is very well described by GT-WAVE while CMEMS underestimates it. Considering the wave period, CMEMS showed a significant underestimation. GT-WAVE performs better, reducing the underestimation of 50%.

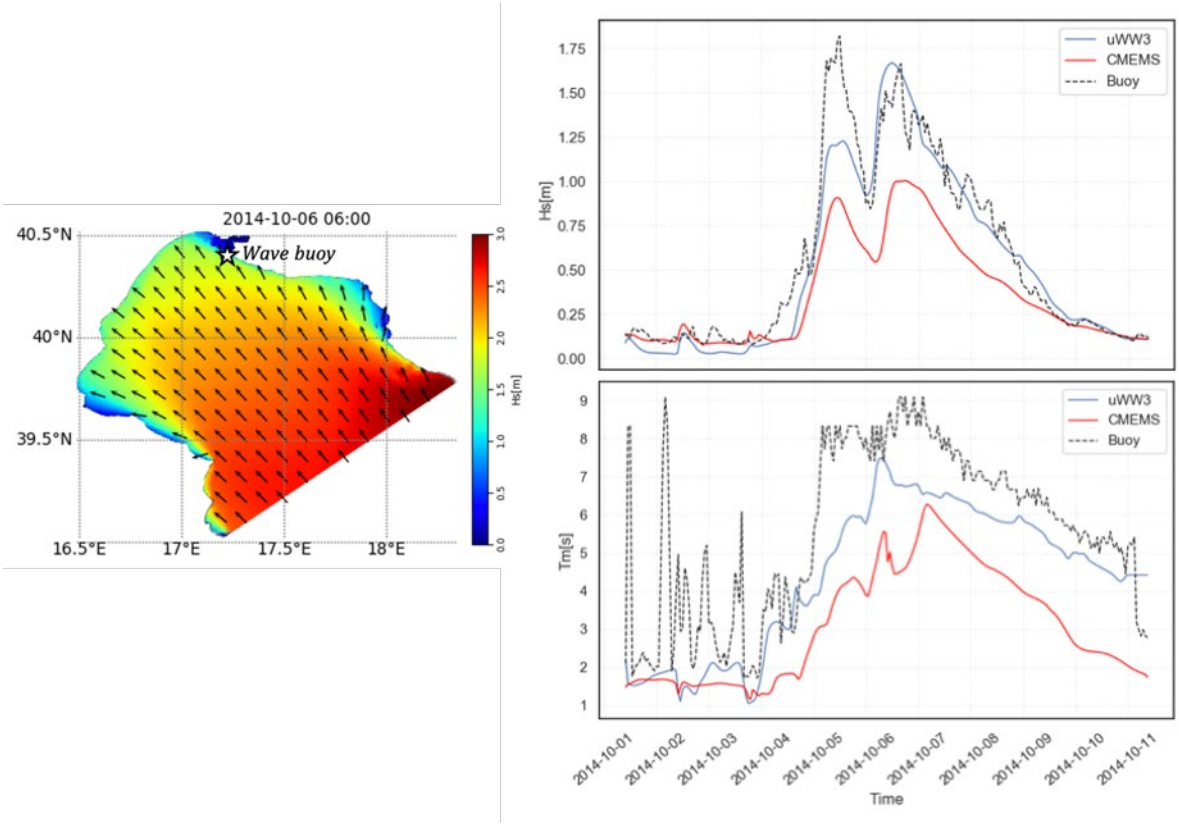

Figure 8. Map of Hs at the peak of the event of October 2014. Models (GT-WAVE and Med-Waves-CMEMS) timeseries of Hs and Tm compared with wave buoy observations.

During the second event, which occurred in the middle of February 2015, the waves entered the open boundary from South. In Figure 9 we report the significant wave map at the highest peak of the event and the timeseries of Hs and Tm during the event. Also, for this case, the event showed 2 peaks respectively on 17th and 23th of February. The first peak, the lowest, reached approximately 2m of Hs, and it was well represented by GT-WAVES. After that, the sea-state restoring phase showed an overestimation of Hs in GT-WAVES, and Hs was better described by CMEMS. The second peak can be considered a real extreme event, with Hs exceeding 3.5m. The event is slightly better described by CMEMS. It is evident that CMEMS tends to underestimate Hs and GT-WAVE tends to overestimate it. The wave period of CMEMS showed a net underestimation, while GT-WAVE is closer to the observed data. For this event we have also performed an assessment of wave-current interaction on total water level. In particular, Figure 10 reports at the peak (2015/02/22 17:00) for the areas of the Taranto port the maps of the significant wave height (top panel), the sea level for the coupled run (middle panel) and the difference in sea level for the coupled and uncoupled runs (bottom panel). Then, in Figure 11, we report the time series of sea level for the coupled and uncoupled configurations together with the significant wave height for a point close to the port (point P1 indicated in Figure 10). The wave contribution (wave setup) to the total water level is clearly evident at the peak of the extreme event.

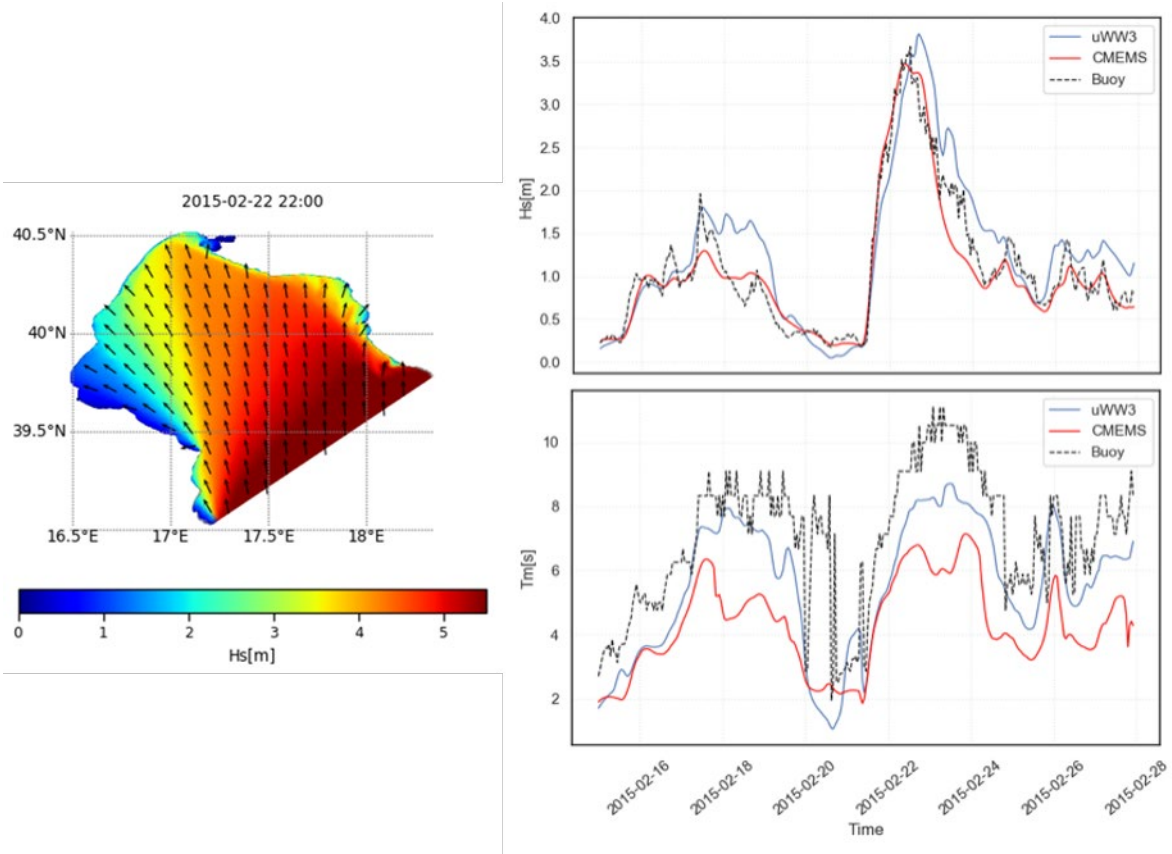

Figure 9. Map of Hs at the peak of the event of February 2015. Models (GT-WAVE and Med-Waves-CMEMS) timeseries of Hs and Tm compared with wave buoy observations.

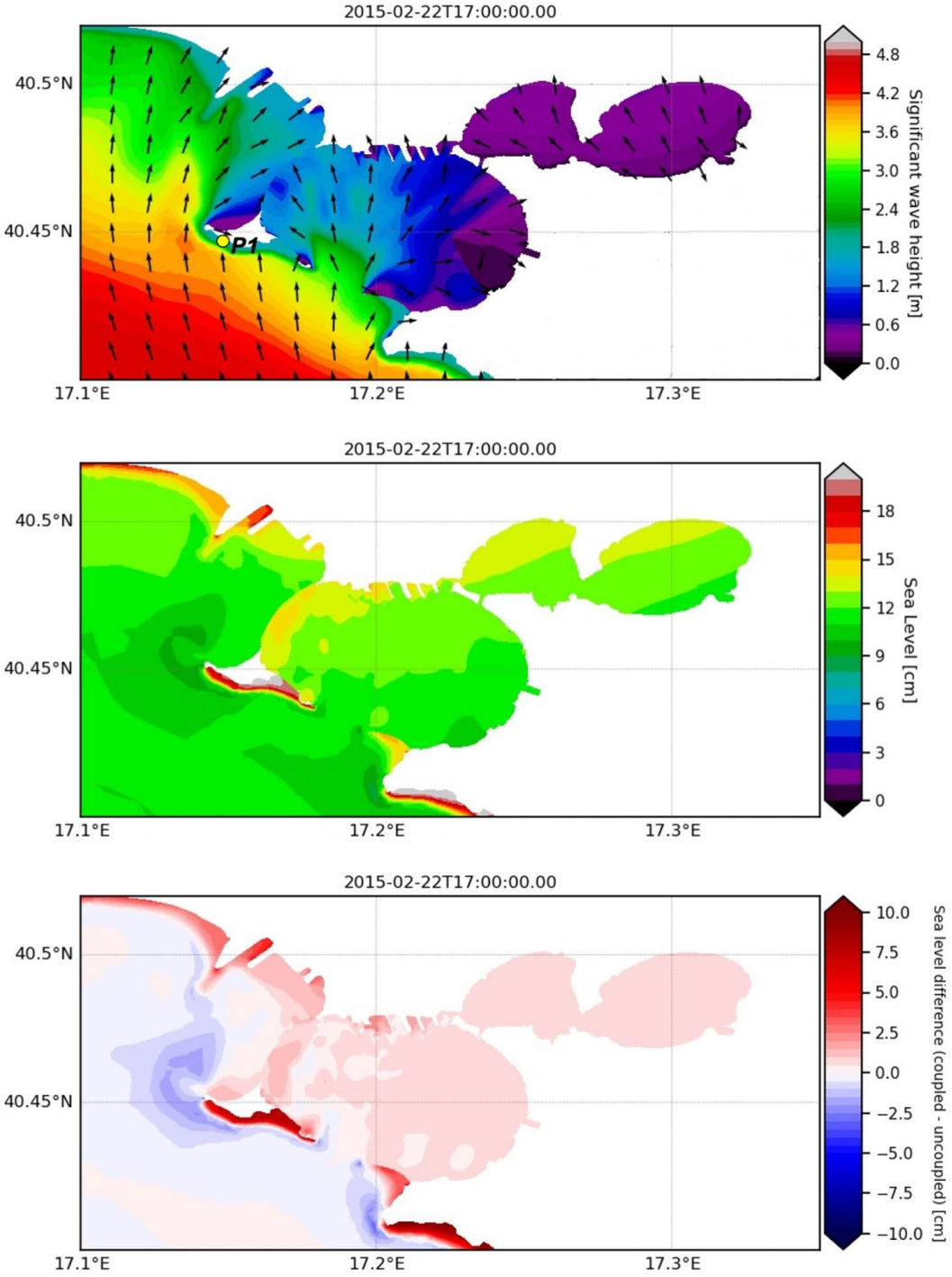

Figure 10. Maps of the significant wave height at the peak of the event of February 2015 (top panel), the sea level for the coupled run (middle panel) and the difference in sea level for the coupled and uncoupled runs (bottom panel).

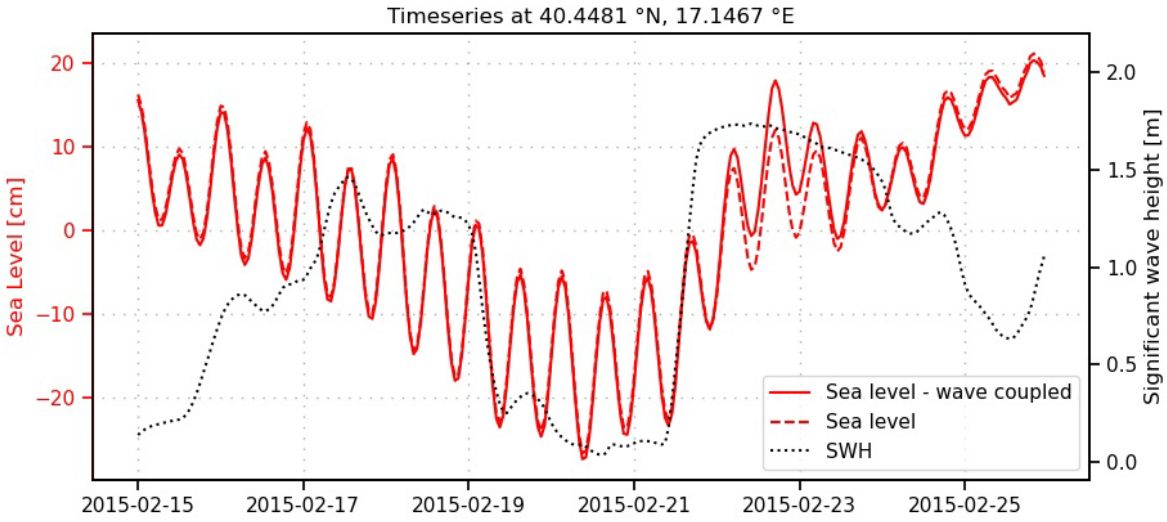

Figure 11. Time series of sea level for the coupled (continuous red line) and uncoupled (dashed red line) configurations together with the significant wave height (point black line) for a point close to the port (point P1 indicated in Figure 10)

The third event occurred in March 2016. In Figure 12 we report the significant wave map at the highest peak of the event and the timeseries of Hs and Tm during the event. During the event two peaks of Hs are present, respectively on 13th and 17th of March 2016. The wave direction approaching the open boundary was S-SE oriented. The first peak (~2.1m) was underestimated by CMEMS, while better represented by GT-WAVE. The second peak (~3.8m) was underestimated by both the models even if GT-WAVE (~3.1m) was closer to observations than CMEMS (~2.8m). Unfortunately, the observation was not complete because of insufficient buoy data on 18th of March. Again, for the mean period the tendency of the previous plots, with both models underestimating the observations, but higher accuracy of GT-WAVE, is confirmed.

We can conclude that GT-WAVE generally performs better than CMEMS for these specific events and in the area. In addiction, we would like to stress that the CMEMS model is also equipped with satellite wave assimilation, while no assimilation is included in the GT-WAVE model.

The GT-WAVE system has been put in operational forecasting mode, providing 3-days of forecasts with hourly frequency. The outputs have been delivered both in unstructured (native) format and regridded format to serve downstream services (e.g. tool for visualization) and applications. The ocean fields released on a daily basis are significant wave height, mean wave period and direction. The operational chain is based on workflow manager with the same features and tools described in the Deliverable 5.3. The forecasting data are included in the OSPAC platform and also displayed at the website[5].

[5] https://taranto.cmcc.it/

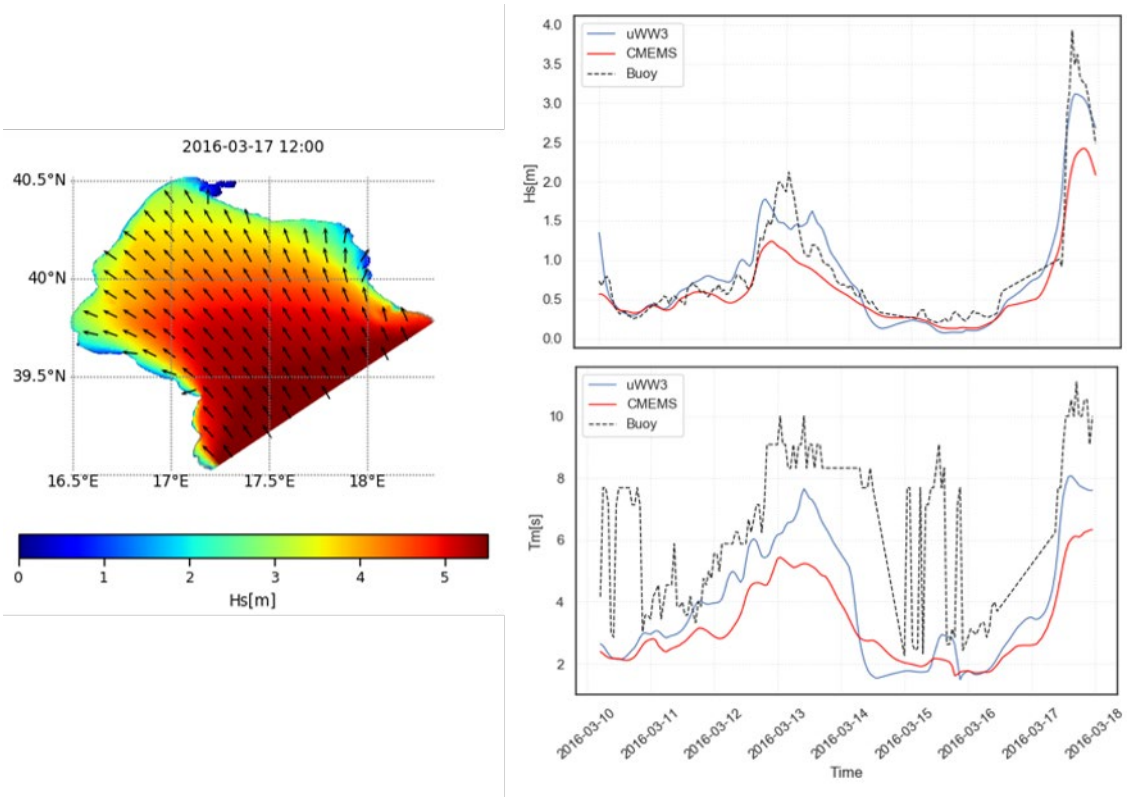

Figure 12. Comparison between wave buoy observations, GT_WAVE and Med-Waves-CMEMS during the extreme events occurred in the middle of March 2016.

Barcelona

The coupled simulation has generated surface fields of significant wave heights, wave direction, wave period, sea level, and other tridimensional oceanographic variables, such as current speeds, temperature or salinity fields. This section will show results in Barcelona's coastal and harbour scale and an analysis comparing the modelling results with observations, especially during extreme wave events (on March 2022).

Figure 13 shows the significant wave height (Hsig) over the entire model domains under storm conditions, with a zoom on the Barcelona port and beaches domain.

The significant wave height shows continuity in all domains, and it is higher in the coastal domain, reaching values greater than 5 meters. In the port domain, these maximum values are 4 meters in some areas; however, the values do not exceed 3 meters in height in the Zoom of Barcelona´s port and beaches.

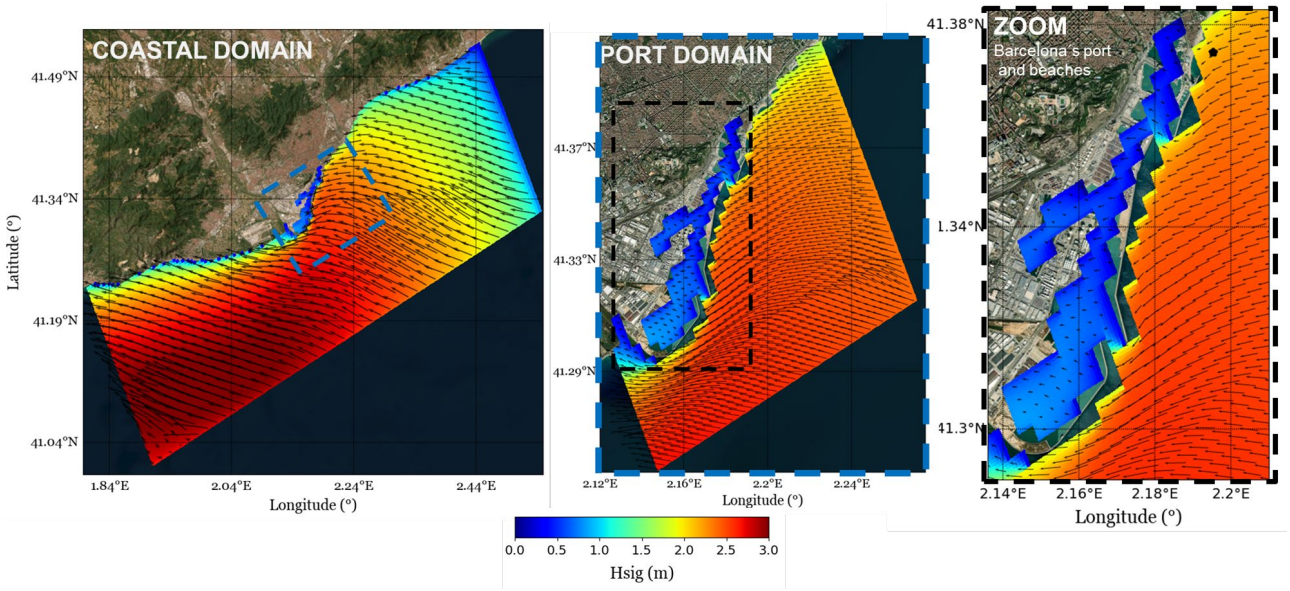

Figure 13. Significant wave height on the Coastal domain (left panel), on the Port domain (central panel) and the Zoom on Barcelona's port and beaches (right panel) under storm conditions (15 March 2022). The black dot indicates the location of the in-situ observations recorded during a field campaign.

Figure 14 shows the significant wave height (Hsig) in a Zoom of the port and the beaches of Barcelona (Domain of the Port), on March 15 2022, at 1:00, 5:00, 10:00, 15:00, 20:00 and 24 hours. This represents a 2D time series of significant wave height variation across the domain during one day. The results in the Zoom show maximum values of significant wave height close to 2 meters in the first hours, which evolve over the hours until they exceed 3 meters (at 10:00 hours) and then descend to values of 1.5 meters.

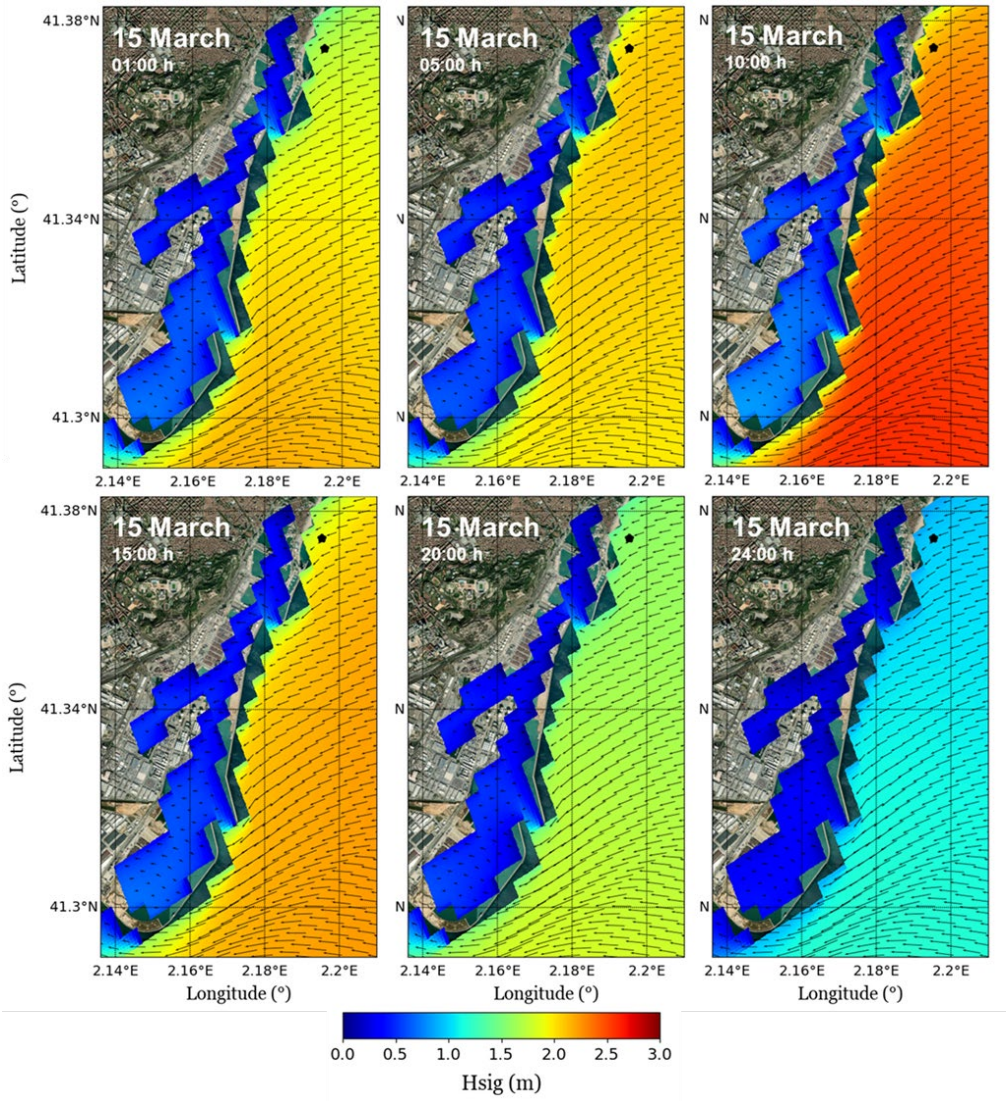

Figure 14. Significant wave height on a Zoom on Barcelona's port and beaches (Port Domain) under storm conditions on 15 March 2022, at 1:00, 5:00, 10:00, 15:00, 20:00 and 24:00 hours. The black dot indicates the location of the in-situ observations recorded during a field campaign.

Product quality assessment is crucial for coupled modelling systems. For that reason, the model outputs have been validated where field data were available (the location of the measurement point is highlighted with a black dot in Figures 13 and 14).

Measurements have been provided by a field campaign led by LIM-UPC between March and April of 2022; during that period, a severe storm called the CELIA storm was recorded, as well as some other big storms with high values of significant wave height. All these data were compared with modelled data. The measuring point was located at 12m of water depth; thus, we were focused on validating only the shallow-water physics in our implementation.

In Figure 15, we report the significant wave height comparison (central panel) where the highest peak of the time series occurred during the CELIA storm on 15 March 2022. It is evident an underestimation of the

modelled results. Still, looking at the rest of the time series, we could say that the model could reproduce reasonably well other Hsig peaks.

The same patterns can be observed with the other two time series, the wind speed (m/s) and the mean sea level (m) (Figure 15, upper panel and lower panel, respectively). The modelled data reproduce the trend and general patterns of the time series, but some peak data are underpredicted.

The correlation between measured and modelled wind speed data, significant wave height data, and mean sea level data is 0.76, 0.73 and 0.71, respectively.

Figure 15. Comparison between measured data (in green) and modelled outputs (in purple) at the black dot location (see Figure 11). The upper panel shows time serie of wind speed (m/s), the central panel shows the time serie of significant wave height (m), and the lower panel shows the time serie of Mean Sea level (m).

Concerning surface current speed data (Figure 16), the coupled model reproduced the trends and patterns shown by measured data, particularly under storm conditions, but underpredicted the peak values along the entire time series. The correlation between measured and modelled surface current speed data is 0.69.

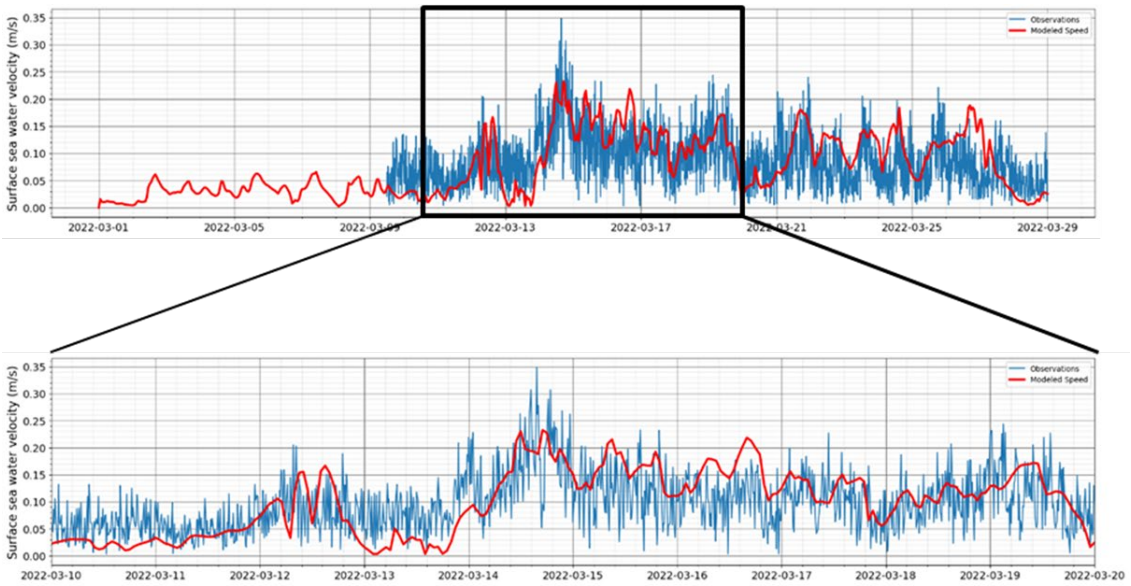

Figure 16. Comparison between measured data (in blue) and modelled outputs (in red) at the black dot location (see Figure 11). The upper panel shows the surface current velocity (m/s), and the lower panel highlight the surface current velocity (m/s) under a specific period of storm conditions.

Finally, Figure 17 (right panel) shows the differences in meters between the significant wave height obtained with the coupled modelling system (left panel) and the results obtained with a wave model (uncoupled, central panel) on a Zoom of Barcelona´s port and beaches (Port Domain).

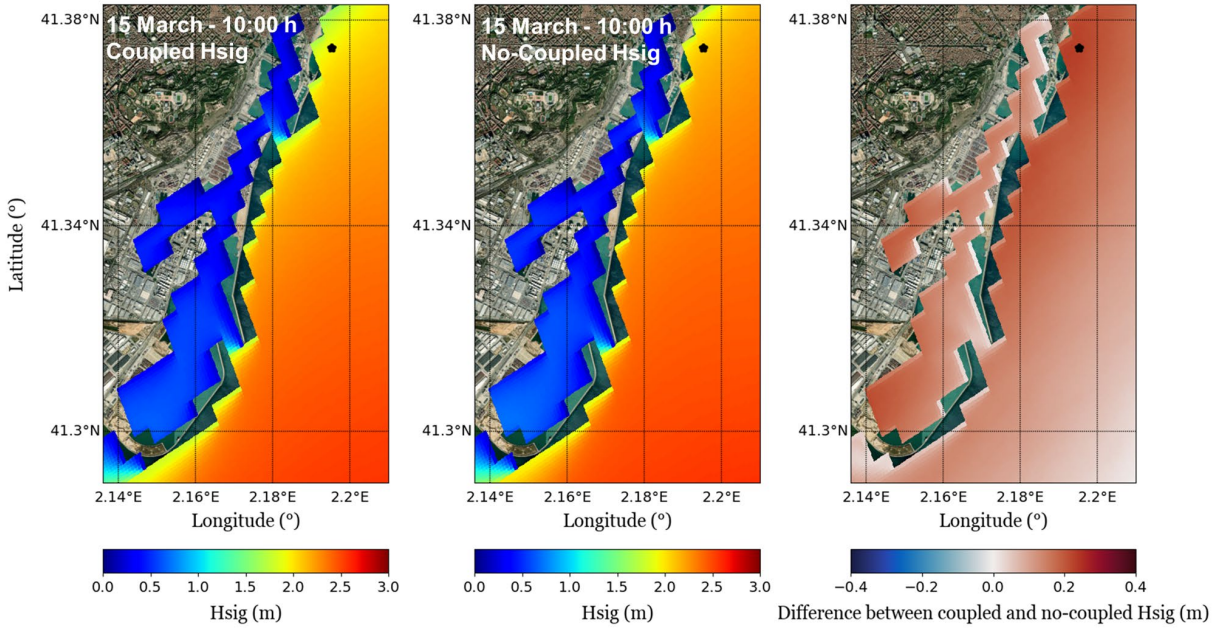

Figure 17. Differences (m) between Significant wave height results from coupled modelling system and no-coupled wave model (right panel), on a Zoom on Barcelona's port and beaches (Port Domain). The left panel shows Hsig (m) from coupled modelling system, and the lower panel shows Hsig (m) from the wave model (no-coupled) on 15 March 2022 at 10:00 hours.

These differences are mainly positive values, which means that the Hsig values obtained with the coupled modelling system are greater than the Hsig values obtained with a wave model (uncoupled). These differences reach 0.4 meters at some points in our study domain.

The coupled modelling system has been tested under different conditions, and results show continuity and agreement between all their variables and parameters. However, although preliminary validations with measured data at shallow waters display good agreements, correlations between them can be improved.

4. Conclusions

Taranto

A wave modelling system based on the unstructured-grid component of WW3 has been implemented for the entire Gulf of Taranto, with the specific focus and higher horizontal resolution (up to 20m) for the Taranto port and embayments. The variable mesh approach ensures continuity and mutual exchanges in seamless fashion among the different scales (sub-regional, coastal and port). The connection with the regional scale of the Mediterranean Sea is performed via downscaling approach based on CMEMS-Med products.

Preliminary sensitivity experiments have been carried out to assess the contribution of shallow water physics in the WW3 model at this coastal-port scale.

The coastal model has been validated over different extreme event conditions and compared against buoy observed data. Furthermore the model has been inter-compared with the CMEMS Med wave model. The coastal model is in agreement with the observed data and is generally capable of better capturing the peak event for significant wave height and mean period.

An assessment of wave-current interaction on total water level has been carried out with coupled and uncoupled experiments, showing the wave contribution (wave setup) to the total water level at the peak of the extreme event in the nearshore and ports areas. One of the main outcomes is that the wave model impacts on the hydrodynamics in the nearshore areas and for extreme surge events, while the contribution becomes negligible for the open ocean and relative calm conditions.

Finally, an operational chain has been implemented to provide every day 3 days of forecasting and the wave characteristics.

Future works will be oriented (i) to the wave-current coupling advancements including further drivers (i.e. air-sea momentum transfer and turbulence induced by waves), and (ii) to the validation of the operational forecasting products.

Barcelona

A coupled wave-current numerical model system was developed and validated with observations and measurements for field campaigns. The coupled model was implemented on the Catalan coast using ROMS and SWAN model codes. The model configuration is nested into the daily updated regional ocean forecast products delivered by CMEMS-IBI. At the sea surface, the models are driven by high frequency (hourly) wind stress, atmospheric pressure, and fluxes of water and surface heat derived from the Spanish Meteorological Agency (AEMET) forecast services.

The coupling consisted of two-way ocean refinement and one-way wave refinement with fully coupled exchanges between two grids for the fields of water levels, currents, bathymetry, and bottom roughness from the ocean to the wave model, and wave dissipation, height, length, direction, surface and bottom periods, and bottom orbital velocities from the wave to the ocean model.

One major conclusion drawn from the various results presented in this work is that this hydrodynamic model coupling impacts the wave model. At the same time, the hydrodynamics changes are negligible in large areas, but they become more evident when considering the coupling impacts during storm events in the nearshore areas, as shown also for the Taranto case.

The uncoupled and coupled wave models perform well in reproducing in situ wave parameters. In addition, the coupled system improves the significant wave height simulation values with respect to the uncoupled system. However, the results also highlight that the enhanced performance of surface currents shows only a minor improvement. This might be due to the low resolution of the hydrodynamic and wave models and, particularly, the scarcity of the coastal areas' geometry and bathymetry. However, although preliminary validations with measured data at shallow waters display good agreements, correlations between them can be improved.

The present work suggests that a two-way coupled model could improve the prediction of wave characteristics and the significant wave height for coastal and local areas, particularly during storm events.

There is still necessary work in the wave model operational implementation to generate quality and accurate forecast results.

References

References for Taranto subsections

Ardhuin, F.; Rogers, E.; Babanin, A.V.; Filipot, J.F.; Magne, R.; Roland, A.; Collard, F. Semiempirical dissipation source functions for ocean waves. Part I: Definition, calibration, and validation. J. Phys. Oceanogr. 2010, 40, 1917–1941.

Battjes, J. A., and J. P. F. M. Janssen (1978), Energy loss and set-up due to breaking of random waves, in Proc. 16th Int. Conf. Coastal Eng., pp. 569–587, ASCE.

Bidlot, J, S Abdalla, and PAEM Janssen (2005). A revised formulation for ocean wave dissipation in CY25R1. In: Internal Memorandum Research Department

Bidlot, JR (2008). Intercomparison of operational wave forecasting systems against buoys: Data from ECMWF, MetO

Chalikov, D. V., and M. Y. Belevich (1993), One-dimensional theory of the wave boundary layer, Bound. Layer Meteor., 63, 65–96.

Damiani, L., Bruno, M.F., Molfetta, M.G.."Coastal zone monitoring in Apulia region: first analysis on meteomarine climate." *Proceedings of the 5th International Symposium on Environmental Hydraulics (ISEH 2007), Tempe, AZ, USA*. 2007.

Eldeberky, Y. (1996), Nonlinear transformationations of wave spectra in the nearshore zone, Ph.D. thesis, Delft University of Technology, Delft, The Netherlands, 203 pp.

Greco, M., & Martino, G. (2014). Assessment of maritime erosion index for Ionian-Lucanian coast. In *Engineering Geology for Society and Territory–Volume 4* (pp. 41-44). Springer, Cham.

Hasselmann, S.; Hasselmann, K.; Allender, J.K.; Barnett, T.P. Computations and parameterizations of the nonlinear energy transfer in a gravity-wave specturm. Part II: Parameterizations of the nonlinear energy transfer for application in wave models. J. Phys. Oceanogr. 1985, 15, 1378–1391.

Hasselmann, D.; Bösenberg, J.; Dunckel, M.; Richter, K.; Grünewald, M.; Carlson, C. Measurements of wave-induced pressure over surface gravity waves. In Wave Dynamics and Radio Probing of the Ocean Surface; Springer: Boston, MA, USA, 1986; pp. 353–368.

Janssen, P. A. E. M. (1991), Quasi-linear theory of of wind wave generation applied to wave forecasting, J. Phys. Oceanogr., 21, 1,631–1,642.

Kara, B. A., Wallcraft, A. J., Hurlburt, H. E., 2007. A Correction for Land Contamination of Atmospheric Variables near Land–Sea Boundaries, *J. Phys. Oceanogr.*, 37, 803–818.

Komen, G. J., S. Hasselmann and K. Hasselmann, 1984: On the existence of a fully developed wind-sea spectrum. J. Phys. Oceanogr., 14, 1,271–1,285.

Korres, G., Ravdas, M., Zacharioudaki, A., Denaxa, D., & Sotiropoulou, M. (2021). Mediterranean Sea Waves Analysis and Forecast (CMEMS MED-Waves, MedWAM3 system) (Version 1) set. Copernicus Monitoring Environment Marine Service (CMEMS). https://doi.org/10.25423/CMCC/MEDSEA_ANALYSISFORECAST_WAV_006_017_MEDWAM3

Liste ,M., Mestres, M., Espino, M., Sanchez-Arcilla, A., García-León, M., G. Sotillo, M., and Alvarez-Fanjul, E. (2021). High-Resolution 3D Forecasting System for Barcelona's Beaches and Coastal Waters. EGU General Assembly. 19-30 April 2021. Vienna, Austria.

Mesinger, F., Janjic, Z. I., Nickovic, S., Gavrilov, D., Deaven, D.G., 1988. The step-mountain coordinate: model description and per- formance for cases of Alpine lee cyclogenesis and for a case of an Appalachian redevelopment, Mon. Weather Rev., 116, 1493– 1518.

Pinardi, N., Lyubartsev, V., Cardellicchio, N., Caporale, C., Ciliberti, S., Coppini, G., De Pascalis, F., Dialti, L., Federico, I., Fil- ippone, M., Grandi, A., Guideri, M., Lecci, R., Lamberti, L., Lorenzetti, G., Lusiani, P., Macripo, C. D., Maicu, F., Mossa, M., Tartarini, D., Trotta, F., Umgiesser, G., Zaggia, L., 2016. Marine Rapid Environmental Assessment in the Gulf of Taranto: a multiscale approach, *Nat. Hazards Earth Syst. Sci.*, 16, 2623–2639

Yamaguchi, M. (1984). Approximate expressions for integral properties of the JONSWAP spectrum. *Doboku Gakkai Ronbunshu*, *1984*(345), 149-152.

References for Barcelona subsections

Ardhuin, F., N. Rascle, and K. Belibassakis (2008), Explicit wave-averaged primitive equations using a generalized Lagrangian mean, Ocean Modell., 20, 35–60, https://doi.org/10.1016/j.ocemod.2007.07.001.

Arnau, P. A., 2000. Aspectos de la variabilidad de mesoescala de la circulación marina en la plataforma continental catalana (Ph.D. thesis). Universitat Poli- tecnica de Catalunya.

Benetazzo, A., Carniel, S., Sclavo, M., Bergamasco, A. (2013). Wave–current interaction: Effect on the wave field in a semi-enclosed basin. Ocean Modelling 70 (2013) 152–165.

Bolaños, R., Jordà, G., Cateura, J., Lopez, J., Puigdefabregas, J., Gomez, J., Espino, M., 2009. The XIOM: 20 years of a regional coastal observatory in the Spanish Catalan coast. J. Mar. Syst.77,237–260.

Ding, Y., and Wang, S.Y. (2011). Modeling of Wave-Current Interaction Using a Multidirectional Wave Action Balance Equation. Coastal Engineering Proceedings. https://doi.org/10.9753/icce.v32.waves.47.

Haidvogel, D. B. , Arango, H.G., Budgell, W. P., Cornuelle, B. D., Curchitser, E., Di Lorenzo, E., Fennel, K., Geyer, W. R., Hermann, A. J., Lanerolle, L., Levin, J., McWilliams, J. C., Miller, A. J., Moore, A. M., Powell, T. M., Shchepetkin, A. F., Sherwood, C. R., Signell, R. P., Warner, J. C., Wilkin, J. (2008). Ocean forecasting in terrain-following coordinates: Formulation and skill assessment of the Regional Ocean Modeling System, Journal of Computational Physics. 227, 3595-3624.

Hashemi, M., and S. Neill (2014), The role of tides in shelf-scale simulations of the wave energy resource, Renewable Energy, 69, 300–310, https://doi.org/10.1016/j.renene.2014.03.052.

Hersbach, H., Bidlot, J.-R. 2008. The relevance of ocean surface current in the ECMWF analysis and forecast system. In: Workshop on Ocean-Atmosphere Interactions, Reading, United Kingdom, European Centre for Medium-Range Weather Forecasts, pp. 61–73.

R. Jacob, J. Larson, and E. Ong, "M×N communication and parallel interpolation in community climate system model version 3 using the model coupling toolkit," The International Journal of High Performance Computing Applications, vol. 19, no. 3, pp. 277–292, 2005.

Liste ,M., Mestres, M., Espino, M., Sanchez-Arcilla, A., García-León, M., G. Sotillo, M., and Alvarez-Fanjul, E. (2021). High-Resolution 3D Forecasting System for Barcelona's Beaches and Coastal Waters. EGU General Assembly. 19-30 April 2021. Vienna, Austria.

Longuet-Higgins, M., and R. Stewart (1964), Radiation stresses in water waves; a physical discussion, with applications, Deep Sea Res. Oceanogr. Abstr., 11, 529–562, https://doi.org/10.1016/0011-7471(64)90001-4.

McWilliams, J., J. Restrepo, and E. Lane (2004), An asymptotic theory for the interaction of waves and currents in coastal waters, J. Fluid Mech., 511, 135–178, https://doi.org/10.1017/S0022112004009358.

Mellor, G. L. (2003), The three-dimensional current and surface wave equations. J. Phys. Oceanogr., 33, 1978–1989.

Mendoza, E.T., Jiménez, J.A., Mateo, J., 2011. A coastal storms intensity scale for the Catalan Sea (NW Mediterranean). Natural Hazards Earth Syst. Sci. 11, 2453–2462.

Mestres M, Grifoll M, Sánchez-Arcilla A. 2016. Analysis of current intensification in the Northwest Mediterranean shelf. Cont Shelf Res. 114:29–40. ISSN 0278-4343, https://doi.org/10.1016/j.csr.2015.12.011.

Pallares, E., Sánchez-Arcilla, A., and Espino, M., 2014. Wave energy balance in wave models (SWAN) for semi-enclosed domains - Application to the Catalan coast. Continental Shel fResearch 87(2014), 41–53. http://dx.doi.org/10.1016/j.csr.2014.03.008.

Poulain, P.-M., Bussani, A., Gerin, R., Jungwirth, R., Mauri, E., Menna, M., Notar-Stefano, G., 2013. Mediterranean surface currents measured with drifters: from basin to subinertial scales. Oceanography 26(1), 38–47. http://dx.doi.org/10.5670/oceanog.2013.03.

Sánchez-Arcilla, A. and Simpson, J., 2002.The narrow shelf concept: couplings and fluxes.Cont. Shelf Res. 22(2), 153–172.

Sánchez-Arcilla, A., González-Marco, D., Bolaños, R., 2008. A review of wave climate and prediction along the Spanish Mediterranean coast. Natural Hazards Earth Syst. Sci. 8, 1217–1228.Shchepetkin, A. F., McWilliams, J.C. (2005). The Regional Oceanic Modeling System: A split-explicit, free-surface, topography-following coordinate oceanic model. Ocean Modeling 9, 347–404. https://doi.org/10.1016/j.ocemod.2004.08.002.

Shchepetkin, A. F., McWilliams, J. C. (2009). Correction and commentary for "Ocean forecasting in terrain-following coordinates: Formulation and skill assessment of the regional ocean modeling system" by Haidvogel et al., J. Comp. Phys. 227, pp. 3595–3624.". Journal of Computational Physics. 228, 8985-9000.

Sotillo, MG., P. Cerralbo, P. Lorente, M. Grifoll, M. Espino, A. Sánchez- Arcilla & E. Álvarez-Fanjul (2019): Coastal ocean forecasting in Spanish ports: the SAMOA operational service, Journal of Operational Oceanography, https://doi.org/10.1080/1755876X.2019.1606765.

Sotillo MG, Cailleau S, Lorente P, Levier B, Aznar R, Reffray G, AmoBaladrón A, Chanut J, Benkiran M, Alvarez-Fanjul E. 2015. The MyOcean IBI ocean forecast and reanalysis systems: operational products and roadmap to the future Copernicus service. J Oper Oceanogr. 8(1):63–79. https://doi.org/10.1080/1755876X.2015.1014663.

Stewart, R.H., Joy, J.W., 1974. HF radio measurements of surface currents. Deep Sea Res. Oceanogr. Abstracts 21, 1039–1049.

Tayfun, M.A., Dalrymple, R.A., Yang, C.Y., 1976. Random wave–current interactions in water of varying depth. Ocean Eng. 3, 403–420.

Tsimplis, M.N., Proctor, R., Flather, R.A., 1995.A two-dimensional tidal model for the Mediterranean Sea. J. Geophys. Res. 100 (C8), 16223–16239. http://dx.doi.org/10.1029/95JC01671.

Warner JC, Sherwood CR, Arango HG, Signell RP. 2005. Performance of four turbulence closure models implemented using a generic length scale method. Ocean Model. 8(1):81–113.